Article citation info:
JAKLIŃSKI P. Analysis of the dual control system operation during failure conditions. Eksploatacja i Niezawodnosc – Maintenance and Reliability 2013; 15 (3): 266–272.

Piotr JAKLIŃSKI

ANALYSIS OF THE DUAL CONTROL SYSTEM OPERATION DURING FAILURE CONDITIONS

ANALIZA DZIAŁANIA DUBLOWANEGO SYSTEMU STEROWANIA W STANACH AWARYJNYCH*

The paper presents an analysis of the ASz-62IR-16E aircraft engine dual control system during failure conditions. The studies which are part of the certification tests in accordance with CS-E are described. The engine was equipped with a prototype electronic fuel injection control system. The experiments were conducted on the ASz-62IR-series piston aircraft engine test stand located in WSK "PZL-Kalisz" S.A. Robustness of the electronic control system has been studied for a single sensor failures and the effects of these failures have been evaluated. The tests included simulated failures of engine speed, manifold air pressure and engine temperature sensors. The results of these tests were described and presented on the time-domain charts. The paper concludes with an analysis and a summary.

***Keywords**: aircraft engine, certification process, bench testing, CS-E.*

W artykule przedstawiono analizę działania dublowanego systemu sterowania silnika lotniczego ASz-62IR-16E w stanach awaryjnych. Opisano badania stanowiące fragment próby dowodowej zgodnej z normą CS-E. Silnik wyposażony był w prototypowy, elektroniczny układ sterowania wtryskiem paliwa. Próby wykonano na stoisku hamownianym silników lotniczych tłokowych ASz-62IR w WSK „PZL-Kalisz" S.A. Badano odporność układu na pojedyncze awarie czujników oraz oceniano skutki tych awarii. Wykonano próby, w których symulowano awarie czujników prędkości obrotowej, ciśnienia powietrza w kolektorze dolotowym i temperatury silnika. Wyniki tych prób opisano i przedstawiono na wykresach przebiegów czasowych oraz przeprowadzono ich analizę. Artykuł zakończono podsumowaniem.

***Słowa kluczowe**: silnik lotniczy, certyfikacja, badania stanowiskowe, CS-E.*

1. Introduction

Safety is the most important requirement imposed on aircraft engines. The engines have to comply with standards which are focused primarily on reliability and robustness to failure conditions. These requirements are contained in the *"Certification Specifications for Engines"* (CS-E) issued by the European Aviation Safety Agency (EASA). For aircraft engine control systems, the standard emphasizes the system's robustness to single failure conditions. The systems are to be designed in such a way as to minimize the possibility of a failure and to mitigate its consequences [1, 7, 13].

One of the commonly applied practices to fulfill those requirements is to use a dual system. These systems are able to operate in parallel or supersede each other. However, the design process of such systems is very complex and demands a series of functional tests to be carried out. There are many different methods and techniques for system safety assessment and life prediction [6, 8, 11, 12, 14]. In this particular case, the correct system operation is definitively proved through a functional test involving failure induction [9, 10].

The targeted project no 04305/C.ZR6-6/2008 „Multi-fuel supply system for ASz-62IR engine", sponsored by the Ministry of Science and Higher Education, completed successfully in 2011. As a result of its realization, the electronically controlled fuel supply and injection system for the ASz-62IR engine was created. The version equipped with the electronic fuel injection system was labeled ASz-62IR-16E and has been undergoing a type certification process since 2010. The requirements of both certification and production preparation processes imposed a substantial series of reliability and durability tests to be carried out, in order to unequivocally demonstrate invulnerability to malfunctions of individual components of the engine equipped with the electronic gasoline injection system.

The ASz-62IR-16E aircraft engine is a 9-cylinder, single-row, air-cooled, radial piston engine with a displacement of 29.87 dm3. The engine underwent numerous constructional and technological modifications since the beginning of its production in 1961. The engine has two valves and two spark plugs per cylinder. It is fuelled by the 100 LL aviation gasoline. The ignition system is composed of two independent ignition subsystems, one per set of spark plugs. The technical specification of the engine are presented in table 1.

The developed electronic fuel injection system is based on the known automotive conception of a multipoint indirect fuel injection, but the control of engine operation is performed in an open loop. The fuel from the central tank is taken by the mechanical fuel pump, filtered and supplied under the correct pressure to the fuel manifold. The fuel is then led to the individual injectors mounted in the inlet pipes of the corresponding cylinders. The fuel pressure is regulated by the pressure regulator, which directs excess fuel back to the tank [4, 5].

For safety reasons, the fuel injection system is a dual system. It is composed of two control subsystems with two independent sets of sensors and one set of actuators - the fuel injectors. The fundamental objective of the design was to ensure that a single failure, be it a failure of a sensor or other system component, cannot adversely affect, or the effect will be negligible, the engine operation. Such assurance is consistent with the requirements contained in the *"Certification Specifications for Engines"* (CS-E) issued by the European Aviation

(*) Tekst artykułu w polskiej wersji językowej dostępny w elektronicznym wydaniu kwartalnika na stronie ***www.ein.org.pl***

Table 1. Technical specification of the ASz-62IR engine

Name	Value
Engine diameter	1380 mm
Length	1130 mm
Dry weight of an engine	567 kg (±2%)
Cylinder diameter	155,5 mm
Piston stroke	174,5 mm
Total displacement	29,911 dm^3
Compression ratio	6,4±0,1
Maximum power at 2200 RPM, Pk=1050 mmHg	1000 KM (735 kW)
Rated power at 2100 RPM, Pk=900 mmHg	820 KM (603 kW)
Rated power at an altitude of 1500 m	840 KM (618 kW)
Power at 2030 RPM, Pk=830 mmHg	738 KM (543 kW)
Power at 1930 RPM, Pk=745 mmHg	615 KM (452 kW)
Power at 1770 RPM, Pk=665 mmHg	492 KM (362 kW)
Average fuel consumption	ca. 200 dm^3/h
Maximum fuel consumption	ca. 330 dm^3/h
Weight to power ratio	0,57 kg/KM (0,42 kg/kW)
Power to displacement ratio	33,43 KM/dm^3 (24,58 kW/dm^3)

Safety Agency. The requirements imposed on the engine control system are described in CS-E 50 [1].

The supplemental type certification process for the ASz-62IR-16E engine involves theoretical analyses and certification tests developed in cooperation with and approved in advance by the certification authority (EASA), including tests carried out during both normal operation of the system and during failure conditions. This meets the requirements set forth in the above-mentioned standards.

2. The objective and scope of research

The purpose of the research was to analyze the operation of the dual control system during failures of selected sensors. These studies were conducted in order to ensure compliance with selected provisions of the CS-E 50 "Engine Control System" [1] with particular emphasis on:

Point (b):

"*(b) Control Transitions. It must be demonstrated that, when a Fault or Failure results in a change from one Control Mode to another, or from one channel to another, or from the Primary System to the Back-up System, the change occurs so that:*

(1) The Engine does not exceed any of its operating limitations,

(2) The Engine does not surge, stall, flame-out or experience unacceptable thrust or power changes or oscillations, or other unacceptable characteristics (...)"

Point (c):

(c) Engine Control System Failures. The Engine Control System must be designed and constructed so that:

(1) The rate for Loss of Thrust (or Power) Control (LOTC/LOPC) events, consistent with the safety objective associated with the intended aircraft application, can be achieved,

(2) In the Full-up Configuration, the system is essentially single Fault tolerant for electrical and electronic Failures with respect to LOTC/LOPC events.

(3) Single Failures of Engine Control System components do not result in a Hazardous Engine Effect,

(4) Foreseeable Failures or malfunctions leading to local events in the intended aircraft installation, such as fire, overheat, or Failures leading to damage to Engine Control System components, must not result in a Hazardous Engine Effect due to Engine Control System Failures or malfunctions."

The scope of the research included certification tests described in the test program, including demonstration of the system robustness to single failures *"failure conditions tests - failure of a single sensor"* and the assessment of the impact of individual failures. The sensors involved in the tests are presented in table 2.

3. Test bench and research methodology

The study was conducted on the ASz-62IR-16E engine test stand located in a WSK „PZL-Kalisz" S.A. facility. The test bench is equipped with measurement devices allowing the tests to be compliant with the provisions imposed by the CS-E. Additionally, as it is practiced by other authors [2, 3, 9], the test bench was equipped with proprietary measurement systems:

1. The diagnostics system allowing to collect and store information about the current operation state of the engine control system 10 times per second;
2. The device allowing to induce failures of individual components during the engine operation – the signal breaker (Fig. 1).

Table 2. Sensors of the control system for the ASz-62IR-16E aircraft engine

Name	Symbol	Type	Manufacturer
Manifold air pressure sensor	MAP	ATM.1ST - 0,22 – 2 pcs	STS Sensor Technik Sirnach AG
Fuel pressure sensor	FP	ATM.1ST - 0,8 – 2 pcs	STS Sensor Technik Sirnach AG
Air temperature sensor	MAT	TP - 371 K-4-22-1000-M2x1.5-SPEC – 2 pcs TP-952-2-2T-SPEC 2x45+120°C/4-20mA (measuring transducer) – 2 pcs	CZAKI Thermo-Product
Fuel temperature sensor	FT	TP - 371 K-4-22-1000-M2x1.5-SPEC – 2 pcs	CZAKI Thermo-Product
Engine temperature sensor	ET	TP - 373 K-1.0-118-SPEC - 2 pcs TP-952-SPEC 2x45+300°C/4-20mA (measuring transducer) – 2 pcs	CZAKI Thermo-Product
Rotational speed sensor	RPM	1GT101DC – 2 pcs	Honeywell International, Inc.
Throttle position sensor	TPS	9851 (clockwise) – 1 pc 9852 (counterclockwise) – 1 pc	BEI Sensors

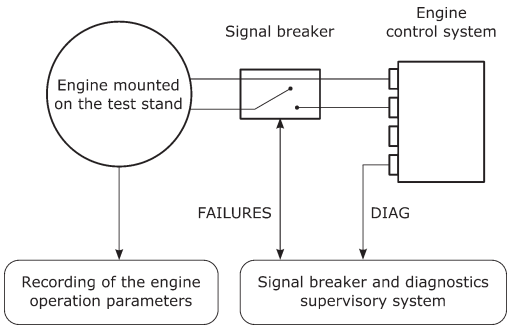

Fig. 1. Overview of the test system

The signal breaker is a device inserted between the engine and the controller. It is designed to physically disconnect electrical circuits connecting the controller to the sensors and injectors.

During the tests, relays embedded in the circuits between the engine harness and the controller were appropriately driven using a computer program. The relays were connected in such a way that the corresponding circuit was connected during the inactive state of the relay. By that means, failures of individual sensors and injectors were simulated.

The signal breaker and diagnostics system were operated with the supervisory system in a form of a PC with special software that allows to induce failures (the FAILURES program) and to record the data sent by the controller (the DIAG program). This allowed to conduct the tests and store the results:

DIAG – the program that allows to register the engine operation by recording measured values, coefficients of the control algorithm and the resulting injection times generated by the controller;

FAILURES - the program that allows to break electrical circuits connecting each sensor and injector to the controller through a physical change of a relay state in the signal breaker.

Table 3. Quantities recorded during the tests

Symbol	Name
t_o	Ambient temperature, °C
B	Ambient pressure, mmHg
ΔB	Absolute humidity, mmHg
t_{pg}	Temperature of inlet air, °C
P_{01}	Oil pressure in the oil pump, kG/cm^2
P_{02}	Oil pressure in the back lid, kG/cm^2
P_{03}	Oil pressure in the reducer, kG/cm^2
P_p	Fuel pressure, kG/cm^2
t_1	Temperature of the oil entering the engine, °C
t_2	Temperature of the oil exiting the engine, °C
t_{head}	Cylinder head temperature, °C
W	Oil flow rate, kg/min
Q	Oil cooling power, kcal/min
n	Crankshaft rotational speed, 1/min
P_k	Manifold air pressure, mmHg
N_{eo}	Power, HP
C_e	Specific fuel consumption, g/KMh
t_{inj}	Fuel injection time, ms
k_{ch}	Cylinder head cooling coefficient, %
t_{fuel}	Fuel temperature, °C
t_{air}	Manifold air temperature, °C
a_{TPS}	Throttle position angle, °

A second, independent recording of the engine operation was performed using the test bench measurement system. The registered values are presented in table 3.

The second, independent measurement recording is required for certification tests compliant with the CS-E.

All tests included a comparison of the engine operation without failure and during a single failure of a chosen sensor at 75% of the nominal engine power defined by the rotational speed n=1910 RPM and manifold air pressure Pk=745±15 mmHg (99.325±2 kPa). During the tests, the engine's operation parameters were continuously recorded. During failure conditions, the injection times, fuel consumption, cylinder head temperatures and output power were measured and evaluated by comparing with the values obtained during normal engine operation. Failure of every sensor was simulated.

In accordance with the control algorithm objectives, a malfunction of a single sensor triggers an automatic detection of an associated failure condition and, as a matter of course, the measurement process is switched from the dual sensor mode to the single sensor mode utilizing only one, operational sensor. This transition may cause a short-lived variation of the time, but not greater than 3% during steady states and 7% during transient states. Variation of output power, fuel consumption and cylinder head temperatures are not expected to exceed 5%.

4. Certification tests

4.1. Failure of the rotational speed sensor

The figure below shows the time plot graph of the injection time and rotational speed measured by both control subsystems during simulated failure of RPM sensor #1 (Fig. 2) and RPM sensor #2 (Fig. 3). Disconnection of the RPM sensor #1 occurred at t=78 s. Disconnection of sensor #2 occurred at t=40 s.

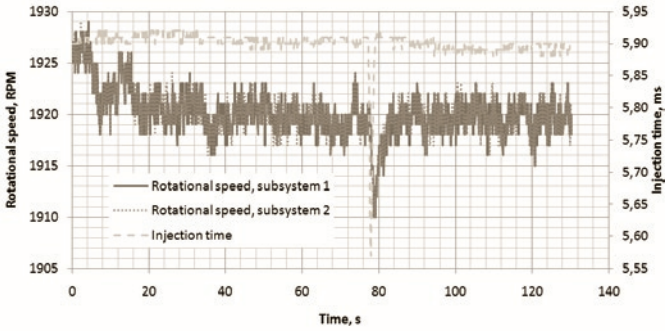

Fig. 2. Injection time and rotational speed during simulated failure of RPM sensor #1

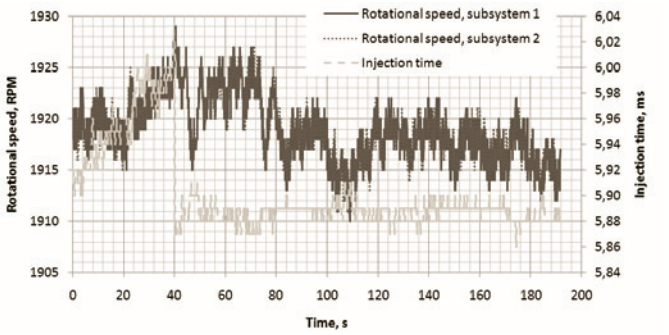

Fig. 3. Injection time and rotational speed during simulated failure of RPM sensor #2

The figures below present the results of the measurements of the engine operating parameters during both normal operation and failure conditions of the RPM sensor #1 (Fig. 4) and sensor #2 (Fig. 5).

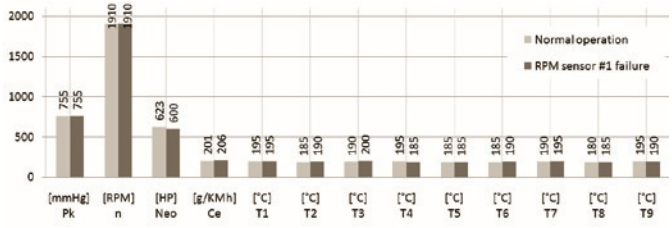

Fig. 4. Measured values of selected engine operation parameters during simulated failure of RPM sensor #1

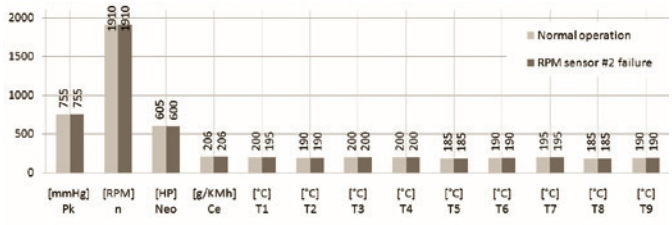

Fig. 5. Measured values of selected engine operation parameters during simulated failure of RPM sensor #2

Both rotational speed sensors included in the control system are triggered by the same tooth of a pulse wheel. Each sensor is connected in parallel to both control subsystems. Due to manufacturing and assembly tolerances, the signals from both sensors are slightly shifted in time. The control algorithm takes into account the earlier signal. Only signals from rotational speed sensors are processed in this manner.

Analysis of the control system operation during failure of RPM sensor #1 shows that failure of the sensor results in a momentary decrease of the rotational speed by 10 RPM and decrease of the injection time by 0.3 ms (which accounts for 5% reduction of the injection time). This state lasts for 2 seconds and after that the system returns to its normal operation. This is confirmed by the results of measurements of the operation parameters of the engine. The failure contributes to a 3.5% reduction of the output power and 2.5% reduction of the specific fuel consumption. The cylinder head temperatures stayed at the same level with variation not exceeding more than 5°C, which in fact is a typical variation for this engine on the test stand.

Analysis of the control system operation during failure of RPM sensor #2 reveals that failure of the sensor results in a momentary decrease of the rotational speed by 5 RPM and increase of the injection time by 0.1 ms (which accounts for 2% increase of the injection time). This state lasted for about 2 seconds. The injection time stabilized immediately after the failure, which is confirmed by the measurements of the engine's operation parameters. The failure contributes to a negligible loss of power (0.8%) without altering the specific fuel consumption. The cylinder head temperatures stayed at the same level with variation not exceeding more than 5°C, which in fact is a typical variation for this engine on the test stand.

4.2. Failure of the manifold air pressure sensor

The control system includes two manifold air pressure sensors, both measuring the same pressure. Each control subsystem is connected to one of the sensors. The values measured by each sensor is exchanged by the subsystem by a means of digital communication link. The control algorithm uses an arithmetic mean based on both values, provided that both values are considered correct by an assessment procedure. When one of the measured values is considered incorrect (e.g. outside a specified range), only the valid one is used. This solution is common for algorithms processing the values obtained from the temperature, pressure and throttle position sensors.

Fig. 6 presents the time plot graphs of the rotational speed and the injection time, whereas fig. 7 shows the signals from both manifold air pressure sensors and the resulting pressure value used for fuel injection time calculation during simulated failure of the MAP sensor #1. The failure condition begins at t=62s and lasts until t=162s.

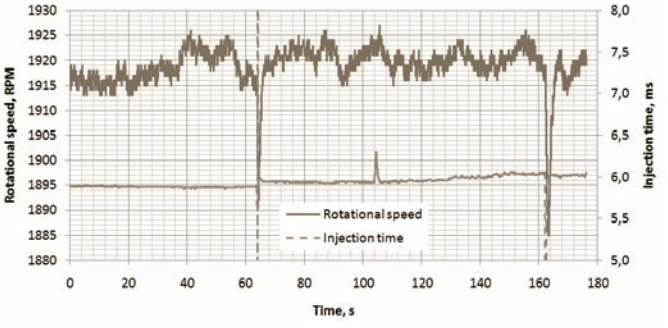

Fig. 6. Injection time and rotational speed during simulated failure of MAP sensor #1

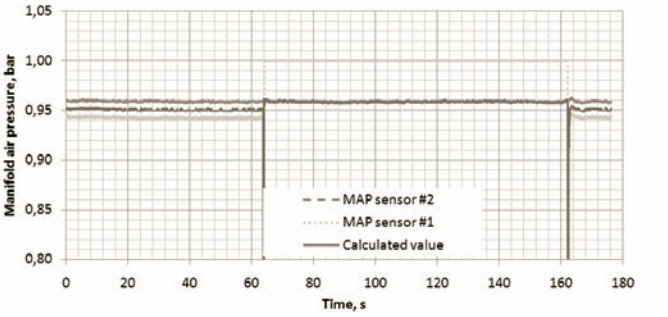

Fig. 7. Measured and calculated values during simulated failure of MAP sensor #1

The results of the measured engine operation parameters during normal operation and the failure state of the MAP sensor #1 are presented in fig. 8.

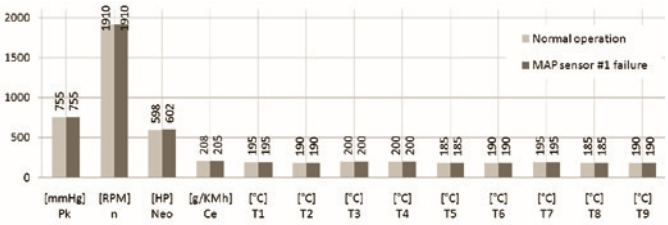

Fig. 8. Measured values of selected engine operation parameters during simulated failure of MAP sensor #1

Fig. 9 presents the time plot graphs of the rotational speed and the injection time, whereas fig. 10 shows the signals from both manifold air pressure sensors and the resulting pressure value used for fuel injection time calculation during simulated failure of the MAP sensor #2. The failure condition begins at t=62 s and lasts until t=158 s.

The results of the measured engine operation parameters during normal operation and the failure state of the MAP sensor #2 are presented in fig. 11.

Failure of the MAP sensor #1 causes the control system to set its corresponding manifold air pressure value with a default value of 1 bar. This value is not used further in fuel injection time calculation. The transition causes a momentary calculation error resulting from averaging of the measured signals. Such a rapid change of the manifold air

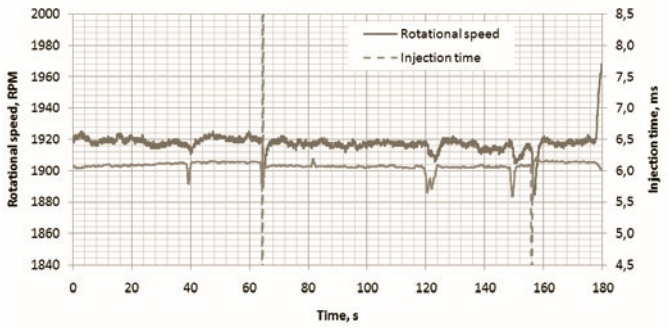

Fig. 9. Injection time and rotational speed during simulated failure of MAP sensor #2

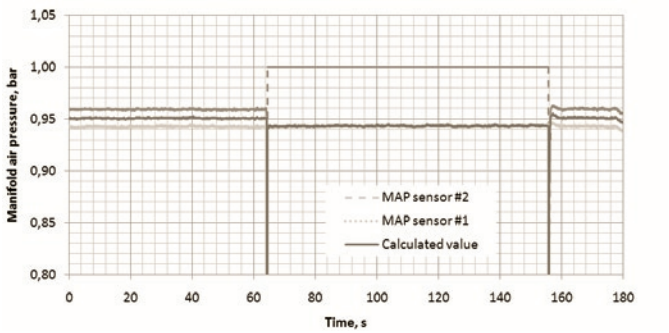

Fig. 10. Measured and calculated values during simulated failure of MAP sensor #2

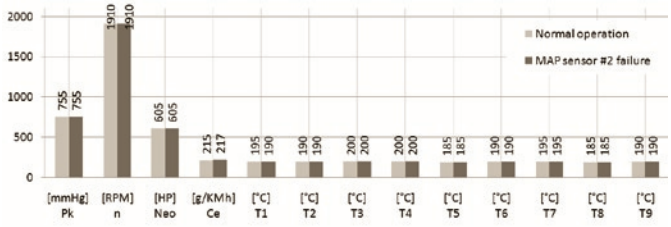

Fig. 11. Measured values of selected engine operation parameters during simulated failure of MAP sensor #2

pressure value influences the fuel film compensation algorithm, which contributes to momentary increase of the injection time to 12 ms, following a decrease to 0 ms in the next cycle. Such behavior is consistent with the design of the control algorithm. This results in a short-lived decrease of the rotational speed by 20 RPM for about 1 second.

During the failure condition, the injection time is increased by 0.1 ms (1.5%). The rotational speed is maintained at a constant level, equal to the engine speed during normal operation.

The recovery from failure condition results in a return of the control algorithm from a single sensor mode back to the dual sensor mode, resulting in an insignificant decrease of the pressure value used in calculations. The transition causes a second execution of the fuel film compensation algorithm, resulting in a one cycle injection cut-off. This is consistent with the design of the control algorithm.

The failure condition of the MAP sensor #1 results in a small increase of the engine output power by 0.5% and decrease of the specific fuel consumption by 1.4%. The temperatures of the cylinder heads remained unchanged.

The failure condition of the MAP sensor #2 results in similar behavior. The state transition causes a momentary error in fuel injection time calculation. Such a rapid change of the measured manifold air pressure manifests itself with a dynamic adjustment of the injection time, resulting in a momentary increase of the injection time to 12 ms, following a decrease to 0 ms in the next cycle. Such behavior complies with the design of the control algorithm. It results with a decrease of the rotational speed by 15 RPM for 1 second.

During the failure condition the injection time is reduced by 0.1 ms (1.5%). The rotational speed is maintained on a constant level, equal to the speed during normal operation of the engine.

The recovery from failure condition results in a return of the control algorithm from a single sensor mode back to the dual sensor mode, resulting in an insignificant decrease of the value used in calculations. The transitions triggers execution of the fuel film compensation algorithm, resulting in a one cycle injection cut-off. This is consistent with the design of the control algorithm.

The failure of the MAP sensor #2 had no measureable impact on the output power. The cylinder head temperatures and specific fuel consumption also remained unchanged.

4.3. Failure of the engine temperature sensor

The control system includes two engine temperature sensors. The ET sensor #1 measures the temperature of cylinder head #2 and the ET sensor #2 measures the temperature of cylinder head #7. The signals from the sensors are processed by external signal measuring transducers and then fed to the corresponding control subsystems. Measured values are different. The control algorithm uses the greater of the two values, provided that both values are considered correct by an assessment procedure.

Fig. 12 presents the time plot graphs of the rotational speed and the injection time, whereas fig. 13 shows the signals from both engine temperature sensors and the resulting temperature value used for fuel injection time calculation during simulated failure of the ET sensor #1. The failure condition begins at t=50 s and lasts until t=152 s.

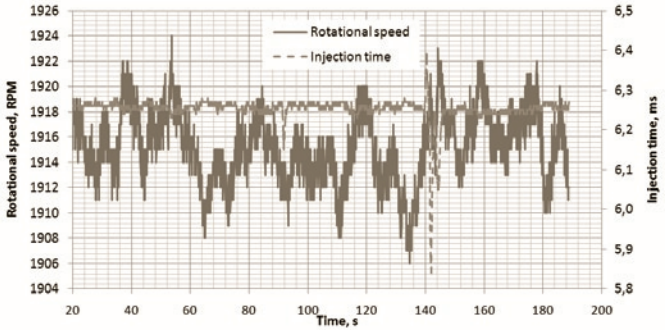

Fig. 12. Injection time and rotational speed during simulated failure of ET sensor #1

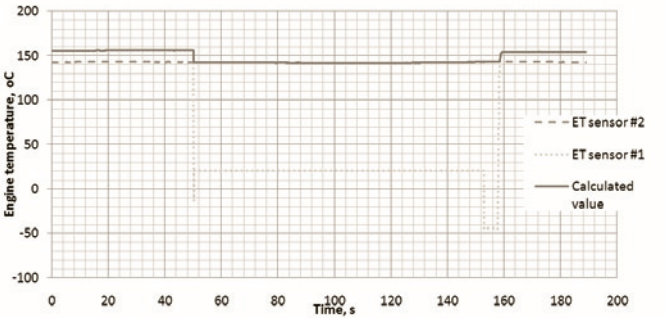

Fig. 13. Measured and calculated values during simulated failure of ET sensor #1

The results of the measured engine operation parameters during normal operation and the failure state of the ET sensor #1 are presented in fig. 14.

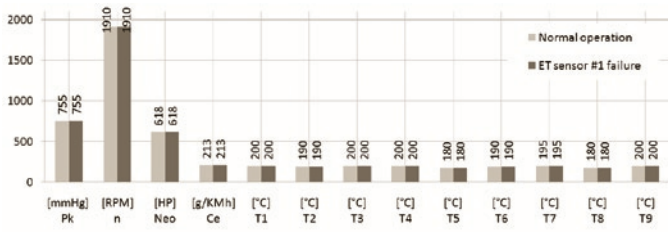

Fig. 14. Measured values of selected engine operation parameters during simulated failure of ET sensor #1

Fig. 15 presents the time plot graphs of the rotational speed and the injection time, whereas fig. 16 shows the signals from both engine temperature sensors and the resulting temperature value used for fuel injection time calculation during simulated failure of the ET sensor #2. The failure condition begins at t=39 s and lasts until t=172 s.

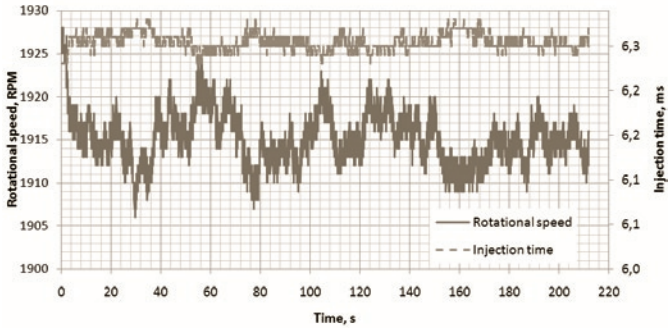

Fig. 15. Injection time and rotational speed during simulated failure of ET sensor #2

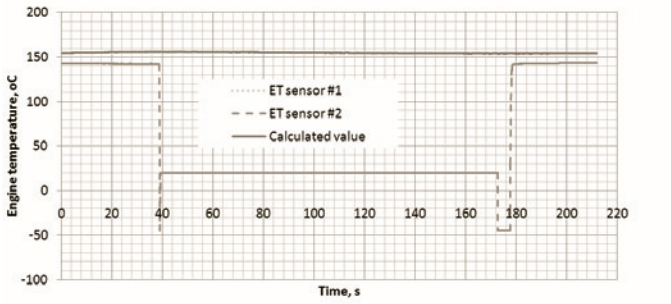

Fig. 16. Measured and calculated values during simulated failure of ET sensor #2

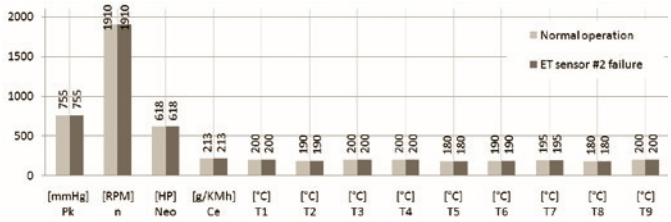

Fig. 17. Measured values of selected engine operation parameters during simulated failure of ET sensor #2

The results of the measured engine operation parameters during normal operation and the failure state of the ET sensor #2 are presented in fig. 17.

Failure of the cylinder head temperature sensor may result in a change of the calculated engine temperature, which is determined by the higher value from both sensors. Due to the nature of the transducer operation, the drop of the measured value is not instantaneous, but takes about 0.5s. Consequently, the response of the control system to the failure condition is delayed until the signal reaches a value outside valid operational range. As the engine temperature value is used by the engine cooling algorithm, the injection time is altered only when the engine temperature is above a certain threshold. This was not the case in the given test, therefore there was no alteration of the injection time.

During the failure condition the engine operates properly and the injection time is consistent with the injection time during fully functional system operation.

During recovery from the failure condition, the sensor and its signal transducer is powered back on, but the transducer is fully operational only after a 7 second delay, which contributes to a significant error in engine temperature's calculation. However, it does not affect the injection time.

The failure condition had no effect on the engine performance. There were no changes in engine power or fuel consumption. The actual cylinder head temperatures also were unchanged.

Since the value measured by the ET sensor #2 was lesser then the ET sensor #1, the calculated engine temperature remained unaffected during ET sensor #2 failure condition, which resulted in no change of the engine performance.

5. Conclusions

Although the described sensors were of various types and each sensor type was utilized in a different manner by the control algorithm, no single failure of any sensor had a negative impact on the engine's operation.

The tests showed that no single sensor malfunction results in loss of engine's performance. The engine and the control system operated properly without going beyond the accepted limits. In most cases, there was no change in engine operation parameters greater than 5% and there was no power output variation beyond acceptable limit.

The tests demonstrated that the requirements contained in CS-E b (1) and (2) were satisfied. During failure conditions there was no engine usability reduction, which satisfies the objectives of CS-E 50 b (1), and there was no engine stall, unwanted oscillations or other unacceptable phenomena, which satisfies CS-E 50 b (2).

The tests proved that the designed control system is completely immune to single sensor failures. In all examined cases, a single sensor failure did not result in a loss of power control, which is required by CS-E 50 c (2).

Simultaneously, the Unsafe Engine Condition did not occur and there was no indication such a possibility could arise, which satisfies the requirements imposed by CS-E 50 c (3), (4).

It can be concluded that the design and control algorithm is insusceptible to a single sensor failure.

References

1. Europejska Agencja Bezpieczeństwa Lotniczego, Specyfikacje Certyfikacyjne dla Silników CS-E, Aneks do Decyzji Dyrektora Wykonawczego 2010/015/R, Zmiana 3, 23 grudnia 2010.
2. Gęca M, Wendeker M, Czarnigowski J, Jakliński P, Nazarewicz A, Pietrykowski K, Barański G. Stanowisko laboratoryjne do badania samolotowego układu wtryskowego. P07-C149, PTNSS Kongres 2007.
3. Gronostajski Z, Hawryluk M, Kaszuba M, Sadowski P, Walczak S, Jabłoński D. Systemy kontrolno-pomiarowe w przemysłowych procesach kucia matrycowego. Eksploatacja i Niezawodnosc – Maintenance and Reliability 2011; 3 (51): 62–69.

4. Jakliński P, Wendeker M, Czarnigowski J, Duk M, Zyska T, Klimkiewicz J. The Indicated Pressure Analyses of Aircraft Radial Piston Engine Fuelled by 100LL and ES95 Gasoline. PTNSS-2009-SC-065, Combustion Engines, Silniki Spalinowe, Special Series 2009-SC2: 162–170.
5. Jakliński P, Wendeker M, Czarnigowski J, Duk M, Zyska T, Klimkiewicz J. The Comparison of the Operating Parameters in an Aircraft Radial Piston Engine Fuelled by 100LL and ES95 Gasoline. PTNSS-2009-SS1-C064, Combustion Engines, Silniki Spalinowe 1/2009: 52–59.
6. Kowalczyk M, Czmochowski J, Rusiński E. Budowa modelu diagnozowania stanów awaryjnych organów roboczych koparki wieloczerpakowej. Eksploatacja i Niezawodnosc – Maintenance and Reliability 2009; 2 (42): 17–24.
7. Lewitowicz J, Kustroń K, Podstawy eksploatacji statków powietrznych cz.1. Warszawa: Wydawnictwo ITWL, 2001.
8. Li Y, Huang H, Liu Y, Xiao N, Li H. Nowa metoda analizy drzewa uszkodzeń; rozmyta analiza dynamicznego drzewa uszkodzeń. Eksploatacja i Niezawodnosc – Maintenance and Reliability 2012; 14 (3); 208–214.
9. Lingaitis LP, Mjamlin S, Baranovsky D, Jastremskas V. Badania eksperymentalne operacyjnej niezawodności eksploatacyjnej silników diesel dla spalinowozów. Eksploatacja i Niezawodnosc – Maintenance and Reliability 2012; 14 (1): 6–11.
10. Olearczuk E, Sikorski M, Tomaszek H. Eksploatacja samolotów (elementy teorii). Warszawa: Wydawnictwo MON, 1978.
11. Pang Y, Huang H, Xiao N, Liu Y, Li Y. Posybilistyczna analiza niezawodnościowa systemu naprawialnego z pominiętym lub opóźnionym efektem uszkodzenia. Eksploatacja i Niezawodnosc – Maintenance and Reliability 2012; 14 (3): 195–202.
12. Wang Z, Huang H, Du X. Projektowanie niezawodnościowe z wykorzystaniem kilku strategii utrzymania. Eksploatacja i Niezawodnosc – Maintenance and Reliability 2009; 4 (44): 37–44.
13. Yu T, Cui W, Song B, Wang S. Ocena wzrostu niezawodności w bezzałogowym statku latającym podczas kolejnych faz badania w locie. Eksploatacja i Niezawodnosc – Maintenance and Reliability 2010; 2 (46): 43–47.
14. Zhou Y, Ma L, Mathew J, Sun Y, Wolff R. Prognozowanie trwałości środków technicznych z wykorzystaniem wielu wskaźników degradacji i zdarzeń awaryjnych w ujęciu modelu ciągłej przestrzeni stanów. Eksploatacja i Niezawodnosc – Maintenance and Reliability 2009; 4 (44): 72–81.

Piotr JAKLIŃSKI, Ph.D. (Eng.)
Department of Thermodynamics, Fluid Mechanics and Aviation Propulsion Systems
Lublin University of Technology
Mechanical Faculty
ul. Nadbystrzycka 38D, 20-618 Lublin, Poland
e-mail: p.jakliński@pollub.pl